Available online at www.sciencedirect.com
SCIENCE DIRECT®
Journal of Power Sources 146 (2005) 645–649
JOURNAL OF POWER SOURCES
www.elsevier.com/locate/jpowsour

Improvement of structural integrity and battery performance of $LiNi_{0.5}Mn_{0.5}O_2$ by Al and Ti doping

Seung-Taek Myung [1], Shinichi Komaba *, Norimitsu Hirosaki, Kiyoharu Hosoya, Naoaki Kumagai

Department of Frontier Materials and Functional Engineering, Graduate School of Engineering, Iwate University, 4-3-5 Ueda, Morioka, Iwate 020-8551, Japan

Available online 25 May 2005

Abstract

$LiNi_{0.5}Mn_{0.5}O_2$, $LiNi_{0.475}Al_{0.05}Mn_{0.475}O_2$, and $LiNi_{0.5}Mn_{0.45}Ti_{0.05}O_2$ were prepared via the emulsion drying method. The as-prepared materials showed different degrees of cation mixing. Rietveld refinement of X-ray diffraction data revealed that Al and Ti doping in $LiNi_{0.5}Mn_{0.5}O_2$ was significantly effective to decrease the cation mixing in the octahedral Li layers. The cation mixing consequently affected to the charge and discharge capacities. The irreversible capacity was the smallest for the Al doped $LiNi_{0.5}Mn_{0.5}O_2$, which showed the smallest cation mixing. Al and Ti doped $LiNi_{0.5}Mn_{0.5}O_2$ delivered a stable capacity of about 175 mAh g^{-1} with high reversibility. Such higher capacities were possible to be obtained by the achievement of structural stabilization and enhancement of structural integrity by Al and Ti doping in $LiNi_{0.5}Mn_{0.5}O_2$.

Keywords: Lithium-ion battery; Cathode; Lithium intercalation; Emulsion drying method

1. Introduction

$LiMO_2$ (M = Co, Ni, Mn) is of great interest for application in rechargeable Li-ion battery system. Even though $LiNiO_2$ exhibits relatively higher capacity, the material shows irreversible phase transitions during charge and discharge, which may cause capacity decrease on cycling. Also, the exothermic decomposition of $LiNiO_2$ in a highly oxidized state at higher temperature (∼200 °C) raises greater safety concerns [1].

Recently, $LiNi_{0.5}Mn_{0.5}O_2$ was introduced by Ohzuku and Makimura [2] and Dahn and coworkers [3]. They suggested that the average oxidation state of Ni and Mn in $LiNi_{0.5}Mn_{0.5}O_2$ are 2+ and 4+, respectively, and the electrochemical reaction is mainly based on $Ni^{2+/4+}$ redox couple between 2.5 and 4.6 V versus Li^0. Because the electrochemically inactive Mn^{4+} provides structural stability by stable electronic configuration like Li_2MnO_3–NiO solid solution, the material shows a stable high capacity of about 150 mAh g^{-1}, good cyclability, and thermal stability upon cycling in the voltage range.

However, it was known that powder preparation of $LiNi_{0.5}Mn_{0.5}O_2$ is not so easy by a conventional ceramic method. In order to synthesize $LiNi_{0.5}Mn_{0.5}O_2$, most of research groups have selected co-precipitation method to prepare double-transition hydroxide, i.e., $Ni_{0.5}Mn_{0.5}(OH)_2$ as a precursor. Purity of a large amount of transition metal doped hydroxide as a precursor played a significant role to decide the quality of the targeted materials.

In this work, the process of the metal double hydroxide preparation was successfully replaced by employing an emulsion drying method, as we reported systematically. Previously, we have successfully prepared the wide solid solution range of spinel type $LiAl_xMn_{2-x}O_4$ [4] and layered $LiMn_xCr_{1-x}O_2$ [5]. Here, we report on powder structural and electrochemistry of layered Al and Ti doped $LiNi_{0.5}Mn_{0.5}O_2$ prepared by the emulsion drying method.

* Corresponding author. Present address: Tokyo University of Science, Shinjuku, Tokyo 162 8601, Japan. Tel.: +81 3 5228 8749; fax: +81 3 5228 8749.
E-mail address: komaba@rs.kagu.tus.ac.jp (S. Komaba).
[1] Present address: VK Corporation, 67 Jije-Dong, Pyongtaek-City, Kyonggi-Do 450-090, South Korea.

0378-7753/$ – see front matter © 2005 Elsevier B.V. All rights reserved.
doi:10.1016/j.jpowsour.2005.03.083

2. Experimental

Al and Ti doped $LiNi_{0.5}Mn_{0.5}O_2$ powders were prepared by the emulsion drying method. We previously reported details of the emulsion drying method [6]. Starting materials used for the synthesis of Al and Ti doped $LiNi_{0.5}Mn_{0.5}O_2$ were $LiNO_3$ (Kanto), $Mn(NO_3)_2{\cdot}6H_2O$ (Kanto), $Ni(NO_3)_2{\cdot}6H_2O$ (Kanto), $Al(NO_3)_3{\cdot}9H_2O$ (Kanto), and $Ti[OCH(CH_3)_2]_4$ (Aldrich). In the starting emulsion, the atomic ratios of Li/(Ni + Mn), Li/(Ni + Mn + Al) and Li/(Ni + Mn + Ti) were 1.25. The obtained powder precursors were preliminary annealed at 400 °C for 6 h in air to oxidize Mn^{II} into Mn^{IV}, because the average oxidation state of starting Mn source was 2+. And then, it was calcined at 950 °C for 12 h in air. The resulting powders were thoroughly washed with distilled water to remove residual lithium salt, then dried at 110 °C. To understand structure of the prepared materials, X-ray powder diffraction (XRD) measurements were carried out using a Kα radiation of Rigaku Rint 2200 diffractormeter. The collected intensity data of XRD were analyzed by the Rietveld refinement program, Fullprof 2000 [7].

For electrode preparation, the prepared powders from the emulsion-dried precursor were mixed with 5 wt.% of graphite, 10 wt.% of acetylene black and 5 wt.% of polyvinylidene fluoride binder in *N*-methyl pyrrolidinone until a slurry was obtained. The slurry was pasted onto Al foil, and the electrodes were dried at 120 °C for 1 h, and then roll-pressed and dried at 80 °C for 1 day under vacuum state. For electrochemical investigation, a coin-type cell (2032) consisted of cathode, lithium foil as an anode, separator and 1 M $LiPF_6$ in ethylene carbonate:diethylcarbonate (2:1 in volume) as an electrolyte. The assembly of the cells was carried out in an Ar-filled glove box. The cells were firstly charged, and then discharged between 4.6 and 2.7 V versus Li^0 with current densities of 20 mA g^{-1} at 25 °C.

In situ XRD data were obtained using a Rigaku Rint 2200 diffractormeter from $2\theta = 10°$ to 70°, with a step size of 0.03° and a count time of 5 s. The in situ cell and attachment were fabricated by Rigaku Inc., with a polypropylene film window fitted in the base of the cell to avoid the corrosion of a conventional beryllium window at higher potentials. The cell was charged and discharged with a current density of 20 mA g^{-1} (C/7). The lattice parameters were calculated by the following method: the positions of the individual peaks were fitted with a psuedo-Voigt or Lorentz function, and typically 30 or 35 peak positions were input to fit the program which minimizes the least-squares difference between the calculated and measured peak positions by adjusting the lattice constant and the vertical displacement of the sample.

3. Results and discussion

Fig. 1 and Table 1 show Rietveld refinement results of XRD patterns of the synthesized powders; $LiNi_{0.5}Mn_{0.5}O_2$, $LiNi_{0.475}Al_{0.05}Mn_{0.475}O_2$, and $LiNi_{0.5}Mn_{0.45}Ti_{0.05}O_2$. The

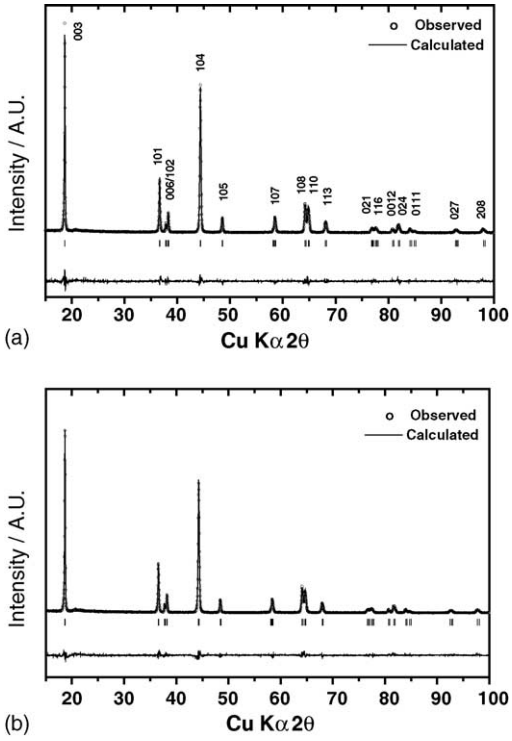

Fig. 1. Rietveld refinement XRD patterns of (a) $LiNi_{0.475}Al_{0.05}Mn_{0.475}O_2$ and (b) $LiNi_{0.5}Mn_{0.45}Ti_{0.05}O_2$ calcined at 950 °C for 12 h in air.

resulting XRD peaks are quite narrow, which indicates high crystallinity. The prepared materials have α-$NaFeO_2$ structure (space group: $R\bar{3}m$) and can be indexed as hexagonal lattice. In all cases, a single phase was observed. From chemical analyses by atomic absorption spectroscopy, it was found that the final products have stoichiometric compositions. For the refinements, it was supposed that Ni^{2+} located at 3a sites can exchange the sites with Li^+ occupied at 3b site due to similarity of their ionic radii (Li^+: 0.69 Å, Ni^{2+}: 0.76 Å [8]). A possibility of the cation mixing was excluded for other elements due to difference in the ionic radii. As can be seen in Fig. 1, the observed and calculated patterns match well for the Al and Ti doped $LiNi_{0.5}Mn_{0.5}O_2$. The integrated intensity ratios of I_{003}/I_{104} were 0.993, 0.984 and 0.955 for Al and Ti doped and undoped ones, that is, the highest was obtained for the Al doped sample in Fig. 1a, which indicates the lower cation mixing as it was also proved by Rietveld refinement in Table 1. This implies that the cation mixing could be suppressed by Al and Ti replacements. According to the Gibbs free energies of the formation at 298 K [9], it is

Table 1
Structural parameters of $LiNi_{0.5}Mn_{0.5}O_2$, $LiNi_{0.475}Al_{0.05}Mn_{0.475}O_2$, and $LiNi_{0.5}Mn_{0.45}Ti_{0.05}O_2$ calcined at 950 °C for 12 h in air

Composition	*a* (Å)	*c* (Å)	Ni^{2+} in Li layer (%)	R_{wp} (%)
$LiNi_{0.5}Mn_{0.5}O_2$	2.887 (7)	14.286 (11)	9.8	13.5
$LiNi_{0.475}Al_{0.05}Mn_{0.475}O_2$	2.875 (2)	14.265 (11)	4.8	11.3
$LiNi_{0.5}Mn_{0.45}Ti_{0.05}O_2$	2.889 (11)	14.300 (15)	5.1	4.70

able to deduce that the metal–oxygen bonding strength would be Al–O > Ti–O > Mn–O > Ni–O. Therefore, the stronger bonding stabilizes the host structure, resulting in enhancement of structural integrity.

Lattice parameters are greatly dependent on the doping elements in Table 1. Al doping resulted in decrease in both *a*- and *c*-axes. On the contrary, Mn replacement by Ti brought about increase in both *a*- and *c*-axes. It is closely related to the ionic radii of dopants; Al and Ti. Ionic radii can be summarize as follow: Li^+ = 0.76 Å, Ni^{2+} = 0.69 Å, Al^{3+} = 0.535 Å, Mn^{4+} = 0.530 Å, Ti^{4+} = 0.60 Å [8]. By consideration of the ionic radii, such variations in lattice parameters in Table 1 are fairly reasonable, obeying Vegard's law. This indicates that the emulsion drying method is effective synthetic method to prepare lithiated transition metal oxides.

Electrochemical properties of the prepared $LiNi_{0.5}Mn_{0.5}O_2$, $LiNi_{0.475}Al_{0.05}Mn_{0.475}O_2$, and $LiNi_{0.5}Mn_{0.45}Ti_{0.05}O_2$ were examined. The charge–discharge profiles between 2.7 and 4.6 V versus Li^0 by applying 20 mA g^{-1} at 25 °C were shown in Fig. 2a–c. As shown in Fig. 2, all the samples initially delivered higher charge capacity over 200 mAh g^{-1}. However, the discharge capacity was dependent on the composition. $LiNi_{0.5}Mn_{0.5}O_2$ had an initial capacity of about 155 mAh g^{-1}. More badly, the capacity gradually faded to 130 mAh g^{-1} by electrochemical cycling. On contrast, Al and Ti doped samples delivered higher discharge capacity of about 175 mAh g^{-1} and the higher capacities were maintained during cycling. The coulombic efficiencies of the first cycle were about 73%, 88%, and 78% for $LiNi_{0.5}Mn_{0.5}O_2$, $LiNi_{0.475}Al_{0.05}Mn_{0.475}O_2$, and $LiNi_{0.5}Mn_{0.45}Ti_{0.05}O_2$, respectively. It seems that such properties are related to cation mixing in the host structure. Because Ni^{2+} ions are located at octahedral Li sites so that the Ni^{2+} ions can block Li^+ intercalation and diffusion. Since the progressive blocking of Li^+ migration by Ni^{2+} in the Li layer exists, as can be seen in Fig. 2a, there was a gradual capacity fading for $LiNi_{0.5}Mn_{0.5}O_2$. For Ni and Ti doped $LiNi_{0.5}Mn_{0.5}O_2$, however, the cation mixing in the Li layer was suppressed effectively so that Li^+ ions would be less blocked by Ni^{2+} ions, resulting in high capacity retention shown in Fig. 2b and c. Therefore, it was found that the enhancement of structural integrity by Al and Ti doping $LiNi_{0.5}Mn_{0.5}O_2$ made possible to be highly reversible Li^+ de-/intercalation during cycling.

Fig. 3 illustrates in situ XRD patterns during the initial charge and discharge for $LiNi_{0.475}Al_{0.05}Mn_{0.475}O_2$, and $LiNi_{0.5}Mn_{0.45}Ti_{0.05}O_2$. For the measurements, a constant current (20 mA g^{-1}) was applied across the cathode. Though the XRD pattern of $LiNi_{0.5}Mn_{0.5}O_2$ was not shown here, the resulting diffraction patterns were similar to that of $LiNi_{0.5}Mn_{0.45}Ti_{0.05}O_2$. One striking feature is the variation in (0 0 *l*) plane of $LiNi_{0.475}Al_{0.05}Mn_{0.475}O_2$ as a function of Li contents, comparing to $LiNi_{0.5}Mn_{0.5}O_2$ and $LiNi_{0.5}Mn_{0.45}Ti_{0.05}O_2$. The plane gradually moved toward lower angle during Li^+ extraction and it reversibly returned to higher angle by Li^+ insertion in Fig. 3a. For $LiNi_{0.5}Mn_{0.45}Ti_{0.05}O_2$, however, the (0 0 *l*) plane first moved to lower angle and one point the plane moved back to higher angle in charge and discharge in Fig. 3b.

Such behaviors can be seen much clearly in the variation in *c*-axis shown in Fig. 4. For Al doped sample, the *c*-axis varies monotonously during Li^+ de-/intercalation. The similar behavior was also observed in Al doped $LiCoO_2$,

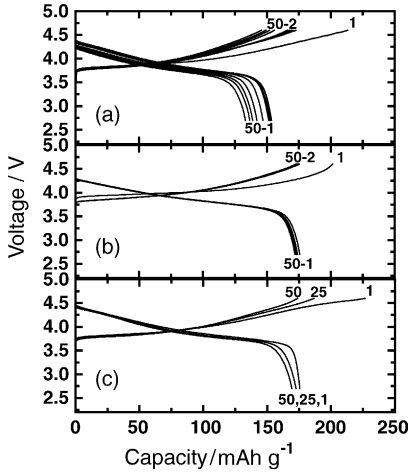

Fig. 2. Continuous charge–discharge curves of (a) $LiNi_{0.5}Mn_{0.5}O_2$, (b) $LiNi_{0.475}Al_{0.05}Mn_{0.475}O_2$ and (c) $LiNi_{0.5}Mn_{0.45}Ti_{0.05}O_2$. The applied current density was 20 mA g^{-1} at 25 °C.

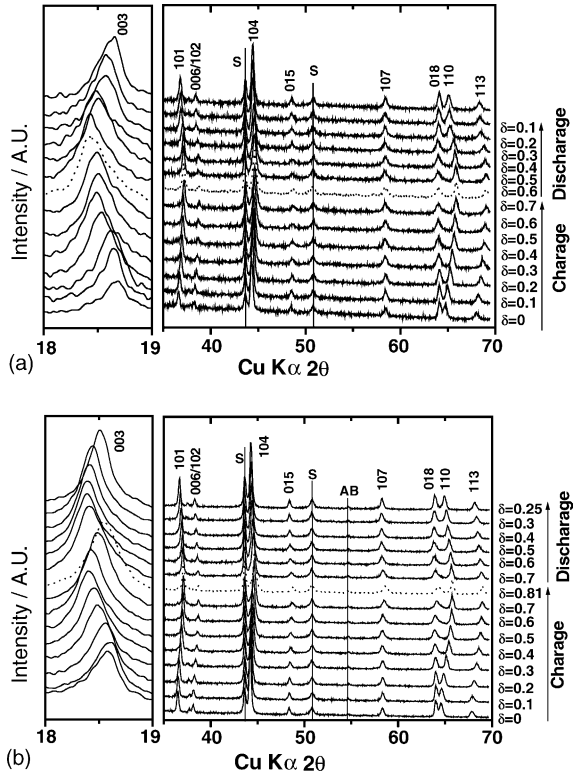

Fig. 3. In situ XRD patterns obtained during the initial deintercalation and intercalation of (a) $Li_{1-\delta}Ni_{0.475}Al_{0.05}Mn_{0.475}O_2$ and (b) $Li_{1-\delta}Ni_{0.5}Mn_{0.45}Ti_{0.05}O_2$. The applied current density was 20 mA g^{-1} at 25 °C.

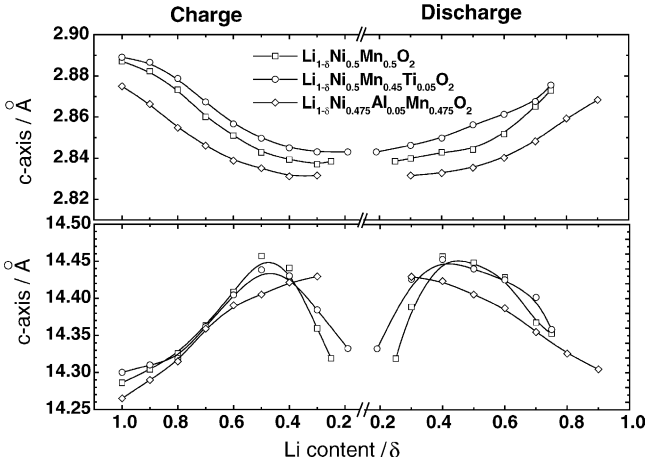

Fig. 4. Variation in lattice parameters of $LiNi_{0.5}Mn_{0.5}O_2$, $LiNi_{0.475}Al_{0.05}Mn_{0.475}O_2$ and $LiNi_{0.5}Mn_{0.45}Ti_{0.05}O_2$ as a function of Li content during the first cycle.

as we previously reported [10]. For $LiNi_{0.5}Mn_{0.5}O_2$ and $LiNi_{0.5}Mn_{0.45}Ti_{0.05}O_2$, however, the *c*-axis constant increased by when 0.5 mol of Li^+ was extracted. Then, the value of axis parameter decreased in the first charge. The similar variation was also observed in Mn based $LiMn_xCr_{1-x}O_2$ [5]. The increase in the *c*-axis parameter is due to the increase in coulombic (electrostatic) repulsion force between oxygen-oxygen layers by ionic bond character. And, the decrease in the c-axis parameter at highly oxidized state is probably due to the formation of covalent bond between transition metal and oxygen resulting in less electrostatic repulsion between the oxygen–oxygen layers to contract the structure so that the *c*-axis parameter decreased drastically at the highly oxidized state. This structural change may be not preferable for cycle life in a practical cell, because the abrupt changes in the *c*-axis would be stressful in the host structure and this, in turn, give rise a gradual or slow capacity fading as shown in Fig. 2a and c, comparing to Fig. 2b. One interesting thing is that the phenomena is observed in the Al doped $LiNi_{0.5}Mn_{0.5}O_2$. Only a small amount of Al doping in $LiNi_{0.5}Mn_{0.5}O_2$ led the ionic bond dominantly during Li^+ de/intercalation process. Other composition also shows ionic bond dominantly [10–12]. Furthermore, the changes in *a*- and *c*-axes were smaller by Al and Ti doping in $LiNi_{0.5}Mn_{0.5}O_2$ in Table 2. It is likely that the bonding energy of M–O would be interacted with the Al and Ti dopings so that the stronger bonding may effect to the constraint of movement of M–O, as we reported the similar effect on spinel $LiAl_xMn_{2-x}O_4$ system [4]. The dramatic changes in the *a*- and *c*-axes may result from the high degree of cation mixing. The reason why Al doped sample shows a strong ionic bond character during charge and discharge is not clear at this time. Further extensive studies are necessary to elucidate this phenomenon.

Table 2
Difference of a and c axes, Δa and Δc, respectively, during the first charging of $LiNi_{0.5}Mn_{0.5}O_2$, $LiNi_{0.475}Al_{0.05}Mn_{0.475}O_2$ and $LiNi_{0.5}Mn_{0.45}Ti_{0.05}O_2$ electrodes

Electrode	Δa (Å)	Δc (Å)
$LiNi_{0.5}Mn_{0.5}O_2$	0.051 (6)	0.171 (14)
$LiNi_{0.475}Al_{0.05}Mn_{0.475}O_2$	0.046 (7)	0.137 (12)
$LiNi_{0.5}Mn_{0.45}Ti_{0.05}O_2$	0.043 (7)	0.165 (9)

4. Conclusion

By calcination of the emulsion-dried precursor at 950 °C for 12 h, it was able to obtain high crystalline $LiNi_{0.5}Mn_{0.5}O_2$, $LiNi_{0.475}Al_{0.05}Mn_{0.475}O_2$, and $LiNi_{0.5}Mn_{0.45}Ti_{0.05}O_2$. Rietveld refinements revealed that the Al and Ti substitution could reduce the cation mixing of $LiNi_{0.5}Mn_{0.5}O_2$. The reduced cation mixing overcame the initial irreversibility, which is one of the main disadvantages of the parent compound. The effect consequently affected to the enhancement on the cycling performances. That is, higher capacities were retained upon cycling for Al and Ti doped $LiNi_{0.5}Mn_{0.5}O_2$. In situ XRD results showed that Al and Ti doped samples resulted in smaller lattice variation during Li^+ extraction and insertion due to the achievement of structural stabilization and enhancement of structural integrity. Therefore, it is concluded that Al and Ti doping in $LiNi_{0.5}Mn_{0.5}O_2$ lattice has positive effect in respect to reduced cation mixing and structural stabilization which consequently effect on improvement on capacity and its retention.

Acknowledgements

The authors would like to thank Ms. N. Kumagai and Mr. S. Takahashi, Iwate University, for their helpful assistance in the experimental work. This study was supported by the program “Development of Rechargeable Lithium Battery with High Energy/Power Density for Vehicle Power Sources” of the Industrial Technology Research Grant Program from the New Energy and Industrial Technology Development Organization (NEDO) of Japan and the Saneyoshi Scholarship Foundation.

References

[1] B. Ammundsen, J.M. Paulsen, Adv. Mater. 13 (2001) 943.
[2] T. Ohzuku, Y. Makimura, Chem. Lett. 2001 (2001) 744.
[3] Z. Lu, L.Y. Beaulieu, R.A. Donaberger, C.L. Thomas, J.R. Dahn, J. Electrochem. Soc. 149 (2002) A778.
[4] S.-T. Myung, S. Komaba, N. Kumagai, J. Electrochem. Soc. 148 (2001) A482.
[5] S.-T. Myung, S. Komaba, N. Hirosaki, N. Kumagai, K. Arai, R. Kodama, I. Nakai, J. Electrochem. Soc. 150 (2003) A1560.
[6] S.-T. Myung, N. Kumagai, S. Komaba, H.-T. Chung, J. Appl. Electrochem. 30 (2000) 1081.
[7] T. Roisnel, J. Rodriguez-Carjaval, Fullprof Manual, Institut Laue-Langevin, Grenoble, 2000.
[8] R.D. Shannon, Acta Crystallogr. A: Cryst. Phys. Diffr. Theor. Gen. Crystallogr. 32 (1976) 751.

[9] G.V. Samsonov, The Oxide Handbook, 2nd ed., IFI/Plenum Inc., USA, 1982, pp. 44–48.
[10] S.-T. Myung, N. Kumagai, S. Komaba, H.-T. Chung, Solid State Ionics 139 (2001) 47.
[11] Y.-I. Jang, B. Huang, H. Wang, D.R. Sadoway, G. Ceder, Y.-M. Chiang, H. Liu, H. Tamura, J. Electrochem. Soc. 146 (1999) 862.
[12] M. Guilmard, C. Pouillerie, L. Croguennec, C. Delmas, Solid State Ionics 160 (2003) 39.